scientific reports

Check for updates

OPEN

# The impact of a humanized bile acid composition on atherosclerosis development in hypercholesterolaemic *Cyp2c70* knockout mice

Tess Yntema[1], Tim R. Eijgenraam[1,2], Niels J. Kloosterhuis[1], Rick Havinga[1], Mirjam H. Koster[1], Milaine V. Hovingh[1], Jan Freark de Boer[1,3], Debby P. Y. Koonen[1,5,6]✉ & Folkert Kuipers[1,4,6]

**Bile acids (BAs) play important roles in the context of lipid homeostasis and inflammation. Based on extensive preclinical mouse studies, BA signaling pathways have been implicated as therapeutic targets for cardiovascular diseases. However, differences in BA metabolism between mice and humans hamper translation of preclinical outcomes. Recently, we generated *Cyp2c70*$^{-/-}$ mice with a human-like BA composition lacking mouse/rat specific muricholic acids. We employed this model to assess the consequences of a human-like BA pool on atherosclerosis and heart function in hypercholesterolaemic mice. We overexpressed a PCSK9 gain-of-function (GOF) mutation in the liver of male *Cyp2c70*$^{-/-}$ and *Cyp2c70*$^{+/-}$ control mice, and fed these mice a Western-type diet (WD) for 12 weeks. *Cyp2c70*$^{-/-}$ mice displayed a hydrophobic BA pool rich in chenodeoxycholic acid. *Cyp2c70*$^{-/-}$ mice showed reduced hepatic total cholesterol and triglycerides ($p < 0.05$) combined with lower plasma total cholesterol ($p < 0.05$) and triglycerides ($p = 0.05$) due to lower VLDL levels. Circulating white blood cells remained largely unaffected in *Cyp2c70*$^{-/-}$ mice. Interestingly, we found a trend ($p = 0.08$) towards smaller atherosclerotic lesions in the aortic root of *Cyp2c70*$^{-/-}$ mice, but no effect on cardiac morphology or function was observed. To conclude, a human-like BA composition ameliorated PCSK9-GOF-induced hypercholesterolaemia in WD-fed mice which translated into a tendency towards smaller atherosclerotic lesions.**

Cardiovascular diseases (CVDs) particularly related to atherosclerosis, represent a leading cause of mortality, taking approximately 18 million lives each year globally[1,2]. Atherosclerosis is a chronic disease of the arterial vessel wall, characterized by inflammatory cell recruitment and the accumulation of lipids[3]. Targeting systemic inflammation and/or hyperlipidemia are currently available treatment strategies to prevent and treat atherosclerosis[3]. Interestingly, preclinical, and clinical studies have shown that alterations in bile acid (BA) metabolism can affect inflammation and hyperlipidemia and are associated with atherosclerosis[4]. Although great efforts have been made to understand the molecular mechanisms and to discover drug targets for atherosclerosis, the link between BA metabolism and atherosclerosis development requires further exploration. BAs, the major catabolic products of cholesterol, aid the absorption of lipid-soluble nutrients in the intestine and emerge as pleiotropic signaling molecules[5]. Human studies have shown that diminished faecal BA excretion is a risk factor for coronary artery disease (CAD)[6]. Excretion of low amounts of BAs (< 415 mg/day) was associated with increased CAD and long-term mortality in CAD patients, conceivably due to impaired ability to remove cholesterol from the body[6]. In addition, preclinical studies have suggested that BAs can regulate cardiovascular function through activation of BA receptors (BAR) (e.g., Farnesoid X Receptor (FXR) and Takeda G-protein-coupled Receptor 5 (TGR5)), muscarinic receptors as well as ion channels in cardiovascular tissue[4].

[1]Department of Pediatrics, University Medical Center Groningen, University of Groningen, Groningen, The Netherlands. [2]Department of Cardiology, University Medical Center Groningen, University of Groningen, Groningen, The Netherlands. [3]Department of Laboratory Medicine, University Medical Center Groningen, University of Groningen, Groningen, The Netherlands. [4]European Research Institute for the Biology of Ageing (ERIBA), University of Groningen, University Medical Center Groningen, Groningen, The Netherlands. [5]Department of Pediatrics, University Medical Center, Groningen. Antonius Deusinglaan 1, Groningen 9713 AV, The Netherlands. [6]Debby P. Y. Koonen and Folkert Kuipers contributed equally. ✉email: d.p.y.koonen@umcg.nl

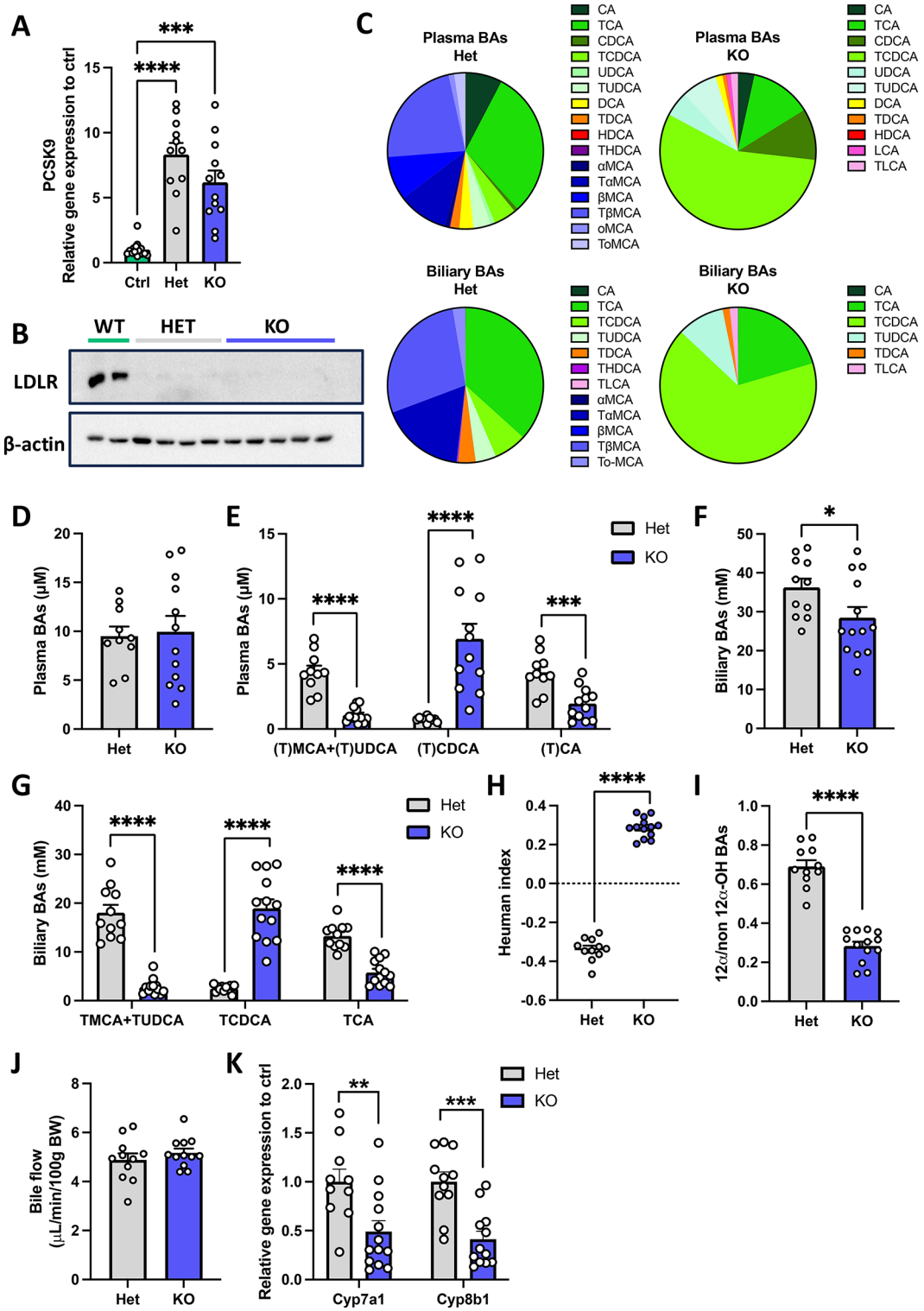


Furthermore, mouse studies have shown beneficial effects of BA signaling on atherosclerosis development[4,7,8]. Interestingly, FXR and TGR5 are expressed in the vasculature and on the plasma membrane of macrophages (FXR)[4]. Activation of these receptors has been shown to attribute to anti-inflammatory[7,8]and/or lipid-lowering[7] effects resulting in atheroprotection in low density lipoprotein receptor knockout (*Ldlr*$^{-/-}$) mice. Although the abovementioned preclinical studies suggest beneficial roles of BAs, the marked species differences in BA composition and metabolism between mice and men hampers the interpretation and translation of these results[9]. Humans synthesize two primary BAs, i.e., cholic acid (CA) and chenodeoxycholic acid (CDCA), in the liver. In mice, the murine specific enzyme CYP2C70 converts CDCA efficiently into muricholic acids (MCAs), which account for ~35% of the total murine BA pool[10]. Because of the hydrophilicity of MCAs, the murine BA pool is much more hydrophilic compared to that of humans. Moreover, different BA species have distinct affinities for activation of FXR and TGR5, with taurine conjugated MCAs even acting as antagonists[11]. Given that also

◀**Fig. 1**. Successful depletion of hepatic LDLR upon AAV-mediated transduction of PCSK9-GOF in *Cyp2c70*$^{-/-}$ mice possessing a hydrophobic BA pool with substantial amounts of CDCA. **(A)** mRNA expression of *PCSK9* in in livers of WT ($n = 15$), and PCSK9-GOF virus injected and WD-fed *Cyp2c70*$^{+/-}$ (Het) and *Cyp2c70*$^{-/-}$ (KO) mice ($n = 11$–13 per group). **(B)** LDLR and β-actin protein levels in livers of WT ($n = 2$), and PCSK9-GOF virus injected and WD-fed *Cyp2c70*$^{+/-}$ ($n = 4$) and *Cyp2c70*$^{-/-}$ ($n = 5$) mice. **(C)** Abundance of BA species in plasma and bile of PCSK9-GOF *Cyp2c70*$^{-/-}$ and *Cyp2c70*$^{+/-}$ mice after 12 weeks of WD. Plasma concentration of **(D)** total BAs and **(E)** (T)MCAs + (T)UDCA, (T)CDCA, and (T)CA in PCSK9-GOF *Cyp2c70*$^{-/-}$ and *Cyp2c70*$^{+/-}$ mice after 12 weeks of WD. Biliary concentration of **(F)** total BAs and **(G)** TMCAs, TCDCA, and TCA in PCSK9-GOF *Cyp2c70*$^{-/-}$ and *Cyp2c70*$^{+/-}$ mice after 12 weeks of WD. **(H)** Hydrophobicity index of biliary BAs, **(I)** ratio of 12α/non-12α-hydroxylated BAs in bile, **(J)** bile flow, and **(K)** hepatic mRNA expression of *Cyp7a1* and *Cyp8b1* in PCSK9-GOF *Cyp2c70*$^{-/-}$ and *Cyp2c70*$^{+/-}$ mice after 12 weeks of WD. Gene expression is normalized to cyclophilin A and depicted as fold change compared to the control group. Data represent mean ± SEM, $^{**}p < 0.01$, $^{***}p < 0.005$, and $^{****}p < 0.0001$ as determined by Kruskal-Wallis followed by Dunn's post hoc test (**A**), Student's T-test (**E-H**, **J**, **K**) or Mann-Whitney U test (**G**) ($n = 11$–13 per group).

the lipid-solubilizing capacity of the human and murine BA pool is different[12], this may differentially affect cardiovascular function. Therefore, we aimed to investigate the effect of a human-like BA pool, lacking MCAs, on atherosclerosis development and heart function in male *Cyp2c70*$^{-/-}$ mice fed a Western-type diet (WD).

## Results

### Expression of a PCSK9-GOF mutant effectively abolished liver LDLR in *Cyp2c70*$^{-/-}$mice with a human-like BA composition

To obtain an atherosclerosis-prone mouse model, we injected male *Cyp2c70*$^{-/-}$ and *Cyp2c70*$^{+/-}$ control mice with adeno-associated virus (AAV) containing a PCSK9 gain-of-function (GOF) mutant. The BA composition and phenotype of *Cy2c70*$^{+/-}$mice are indistinguishable from those of wild-type (WT) mice[9], and therefore serve as controls. Following AAV injection, mice were subjected to a WD for 12 weeks. As expected, injection with AAV-PCSK9-GOF resulted in a significant increase in PCSK9 mRNA expression in the livers of *Cyp2c70*$^{-/-}$ (KO) and *Cyp2c70*$^{+/-}$ (Het) mice compared to untreated WT mice (Fig. 1A). This was associated with a massive reduction in the hepatic expression of the low-density lipoprotein receptor (LDLR) in both *Cyp2c70*$^{-/-}$ and *Cyp2c70*$^{+/-}$ mice compared to WT mice (Fig. 1B, Supplemental Fig. S1).

To confirm a shift in BA composition due to absence of CYP2C70, we measured BAs in plasma and bile (Fig. 1C-G). Indeed, MCAs were completely absent in plasma and bile (Fig. 1C), while CDCA-derived BAs were substantially increased in plasma and bile of *Cyp2c70*$^{-/-}$ mice compared to *Cyp2c70*$^{+/-}$ mice at the expense of CA-derived BAs (Fig. 1E, G). As a result of the altered abundance of BA species, the hydrophobicity index of biliary BAs was increased in *Cyp2c70*$^{-/-}$mice ($\approx +0.2$) compared to control mice ($\approx -0.3$) to a level that is comparable to human bile ($\approx +0.3$)[13] (Fig. 1H). CYP2C70 ablation also resulted in a reduced ratio of 12α/non-12α-hydroxylated BAs in bile (CA- versus CDCA-derived BAs) (Fig. 1I), it did not affect bile flow (Fig. 1J) and BA synthesis genes *Cyp7a1* and *Cyp8b1* were decreased in the liver (Fig. 1K). Altogether, these data confirmed a more human-like BA pool in *Cyp2c70*$^{-/-}$ mice and efficient PCSK9-GOF-induced knockdown of LDLR in livers of both *Cyp2c70*$^{-/-}$ and *Cyp2c70*$^{+/-}$ mice.

### WD feeding resulted in the attenuation of fatty liver, accompanied by elevated liver damage markers in *Cyp2c70*$^{-/-}$ mice

Throughout the experiment body weight (Fig. 2A, Supplemental Fig. S2A) and food intake (Supplemental Fig. S2B) were not affected by the absence of CYP2C70, and body composition was similar between groups after 12 weeks of WD (Supplemental Fig. S2C). Since liver disease is associated with CVD[14], we investigated liver damage markers in *Cyp2c70*$^{-/-}$ mice. The liver weight was lower in *Cyp2c70*$^{-/-}$ mice compared to *Cyp2c70*$^{+/-}$ mice (Fig. 2B), whereas plasma levels of liver transaminases were elevated upon *Cyp2c70* deletion (Fig. 2C). Although H&E staining of liver sections revealed clear peri-central lipid accumulation after 12 weeks of WD in both *Cyp2c70*$^{-/-}$ and *Cyp2c70*$^{+/-}$ mice (Fig. 2D), hepatic triglycerides (TG) were significantly reduced in *Cyp2c70*$^{-/-}$ compared to *Cyp2c70*$^{+/-}$ mice (Fig. 2E). This was accompanied by a prominent reduction in hepatic total cholesterol (TC) and cholesteryl esters (CE) (Fig. 2F, G, $p < 0.005$), resulting in a slight reduction in the ratio of esterified to total cholesterol in *Cyp2c70*$^{-/-}$ versus *Cyp2c70*$^{+/-}$ mice (Fig. 2H, $p < 0.05$). Sirius Red staining showed no substantial fibrosis in the livers of *Cyp2c70*$^{-/-}$ and *Cyp2c70*$^{+/-}$ mice, without prominent differences between groups (Fig. 2D). Thus, these findings indicate that WD-induced fatty liver is mitigated despite elevated liver damage in *Cyp2c70*$^{-/-}$ mice.

### Plasma lipids and circulatory monocytes were reduced in *Cyp2c70*$^{-/-}$ mice

Next, we investigated other risk factors of atherosclerosis, including hyperlipidemia and systemic inflammation. Strikingly, total plasma cholesterol ($p < 0.05$) and triglyceride ($p = 0.053$) levels were decreased in *Cyp2c70*$^{-/-}$ mice compared to *Cyp2c70*$^{+/-}$ mice (Fig. 3A). Whereas LDL-cholesterol seemed to be slightly increased, very-low-density lipoprotein (VLDL)-cholesterol levels were reduced in plasma of *Cyp2c70*$^{-/-}$ mice compared to controls (Fig. 3B). There were no differences in expression of hepatic genes encoding enzymes involved in cholesterol synthesis and lipogenesis (HMG-CoA Reductase, *Hmgcr*; Sterol Regulatory Element-Binding Protein 1, *Srebf1*; Acetyl Coenzyme A Carboxylase 1, *Acaca*; Fatty Acid Synthase, *Fasn*; Diacylglycerol O-acyltransferase 1- and 2, *Dgat1*, and *Dgat2*) in *Cyp2c70*$^{-/-}$ mice compared to control mice (Supplemental Fig. S3A). Apart from a slight, but significant reduction in hepatic ATP Binding Cassette Subfamily G Member 5 (*Abcg5*) mRNA expression

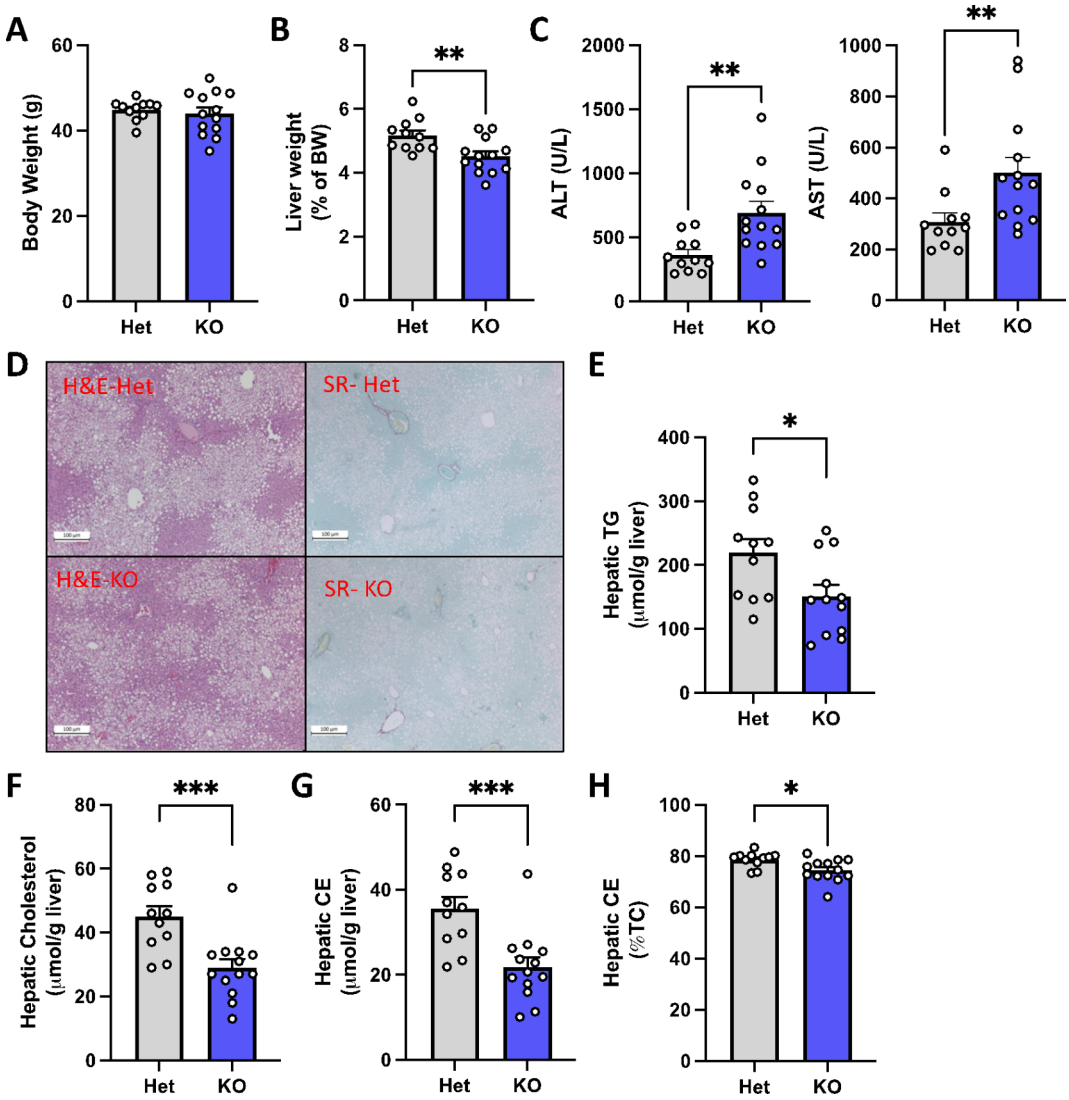


**Fig. 2**. Diminished lipid accumulation with mild liver damage in *Cyp2c70*$^{-/-}$ mice. **(A)** Body weight and **(B)** liver to body weight ratio of PCSK9-GOF *Cyp2c70*$^{-/-}$ and *Cyp2c70*$^{+/-}$ mice after 12 weeks of WD feeding. **(C)** Plasma alanine transaminase (ALT) and aspartate aminotransferase (AST) levels. **(D)** Representative images of liver sections stained with haematoxylin and eosin, and sirius red (scale bar = 100 µm). **(E)** Hepatic triglyceride (TG) levels in *Cyp2c70*$^{-/-}$ and *Cyp2c70*$^{+/-}$ mice after 12 weeks of WD feeding. **(F)** Hepatic total cholesterol levels in *Cyp2c70*$^{-/-}$ and *Cyp2c70*$^{+/-}$ mice after 12 weeks of WD feeding. **(G, H)** Hepatic cholesteryl ester levels in *Cyp2c70*$^{-/-}$ and *Cyp2c70*$^{+/-}$ mice after 12 weeks of WD feeding. Data represent mean ± SEM, $^{*}p < 0.05$, $^{**}p < 0.01$ and $^{***}p < 0.005$, as determined by Student's T-test (**B**, **C**, **E**, **H**) and Mann-Whitney U test (**C**, **F**, **G**) ($n = 11$–$13$ per group).

in *Cyp2c70*$^{-/-}$ mice compared to *Cyp2c70*$^{+/-}$ mice, no further differences were observed in genes encoding enzymes involved in bile acid and cholesterol transport ($Na^{+}$-taurocholate cotransporting polypeptide; NTCP, ATP Binding Cassette Subfamily G Member 8; *Abcg8*, bile salt export pump; *Bsep*) (Supplemental Fig. S3B).

Spleen weight (Fig. 3C) and circulating white blood cells (WBCs) (Fig. 3D) did not differ between *Cyp2c70*$^{-/-}$ mice and controls. Particularly, absolute numbers of neutrophils, monocytes, and their subsets (proinflammatory Ly6C high and patrolling Ly6C low) were similar between groups (Fig. 3E). Only the percentage of monocytes relative to the total numbers of leukocytes was reduced in *Cyp2c70*$^{-/-}$ mice compared to their control counterparts (Fig. 3F). Thus, *Cyp2c70*$^{-/-}$ mice displayed reduced plasma lipids and limited effects on circulating WBCs.

## Plaque formation was delayed in the early atherosclerotic phase of *Cyp2c70*$^{-/-}$ mice

After investigating the involvement of a human-like BA pool on traditional risk factors of CVD, we analysed atherosclerotic plaque lesions in the aortic root, and we determined the heart function of *Cyp2c70*$^{-/-}$ mice. We observed relatively small atherosclerotic lesions in both *Cyp2c70*$^{-/-}$ and *Cyp2c70*$^{+/-}$ mice after 12 weeks of WD feeding, representing the *initiation* phase of disease development. Although we found a trend towards smaller atherosclerotic lesions in *Cyp2c70*$^{-/-}$ mice compared to controls ($p = 0.0812$) (Fig. 4A and B), the relative

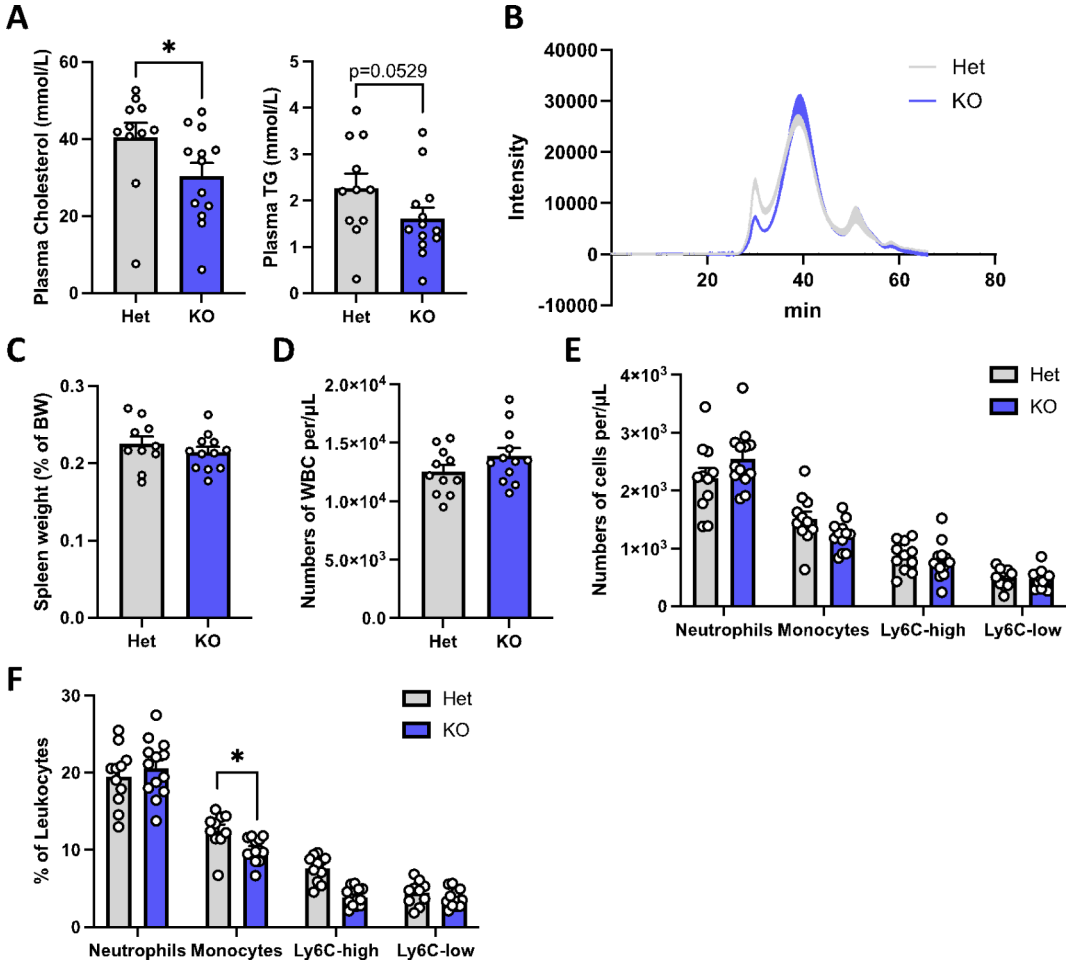


**Fig. 3**. Decreased plasma VLDL-cholesterol levels and limited effects on circulating white blood cells in *Cyp2c70*$^{-/-}$ mice. **(A)** Total plasma cholesterol levels and triglyceride (TG) levels. **(B)** Cholesterol distribution after lipoprotein fractionation of plasma sample by fast protein liquid chromatography. **(C)** Spleen weight to body weight ratio. **(D)** White blood cells count. **(E)** White blood cells subsets count and **(F)** percentage of blood leukocyte levels of *Cyp2c70*$^{-/-}$ and *Cyp2c70*$^{+/-}$ mice after 12 weeks of WD. Data represent mean ± SEM, $^{*}p < 0.05$ as determined by Mann-Whitney U test (**A**, **F**) ($n = 11–13$ per group).

area of MAC2-positive cells (pro-inflammatory macrophages) in plaques remained unaffected upon *Cyp2c70* ablation (Fig. 4C). Finally, echocardiographic analysis demonstrated similar cardiac morphology and function in *Cyp2c70*$^{-/-}$ mice and *Cyp2c70*$^{+/-}$ mice as heart rates, left ventricular end-systolic and end-diastolic internal diameters, and fractional shortening were not different between groups (Fig. 4D-F). Taken together, the human-like BA pool of *Cyp2c70*$^{-/-}$ mice appeared to delay the initiation of WD-induced atherosclerosis upon PCSK9-mediated depletion of hepatic LDLR.

## Discussion

In this study, we assessed the consequences of Cyp2c70-deletion on atherosclerosis development and heart function in male *Cyp2c70*$^{-/-}$ mice expressing a PCSK9-GOF mutant and fed a WD for 12 weeks. The human-like BA composition led to mild liver damage, reduced hepatic and plasma lipid levels and a trend towards smaller lesions in the initiation phase of atherosclerosis development. To validate our model, we confirmed that *Cyp2c70*$^{-/-}$ mice possess a human-like BA composition, lacking MCAs and containing a high abundance of CDCA. As a result of the changes in BA composition, the hydrophobicity index of biliary BAs was increased in *Cyp2c70*$^{-/-}$ ($\approx +0.2$) compared to *Cyp2c70*$^{+/-}$ mice ($\approx -0.3$). The hydrophobicity of BAs of *Cyp2c70*$^{-/-}$mice closely resembles that of humans ($\approx +0.3$)[13]. In line with others, hepatic genes *Cyp7a1* and *Cyp8b1* were reduced in *Cyp2c70*$^{-/-}$mice[9,15]. The high abundance of CDCA in the BA pool of *Cyp2c70*$^{-/-}$mice, which is a potent endogenous FXR activator[16], results in more FXR agonists in the pool of *Cyp2c70*$^{-/-}$ mice compared to control mice. Studies have shown that FXR-related genes are upregulated in the ileum of *Cyp2c70*$^{-/-}$ mice, while Fibroblast growth factor 15 (*Fgf15*), an important protein in the control of hepatic synthesis, remained unaffected[9,15]. In this present study, ileal *Fgf15* expression was significantly reduced in *Cyp2c70*$^{-/-}$ mice (Supplemental Fig. S3C) and thus cannot explain the observed downregulation in *Cyp7a1* and *Cyp8b1* in *Cyp2c70*$^{-/-}$ mice (Fig. 1K). Instead, this may be related to the induction of hepatic inflammation which was shown to be dependent on the concentration

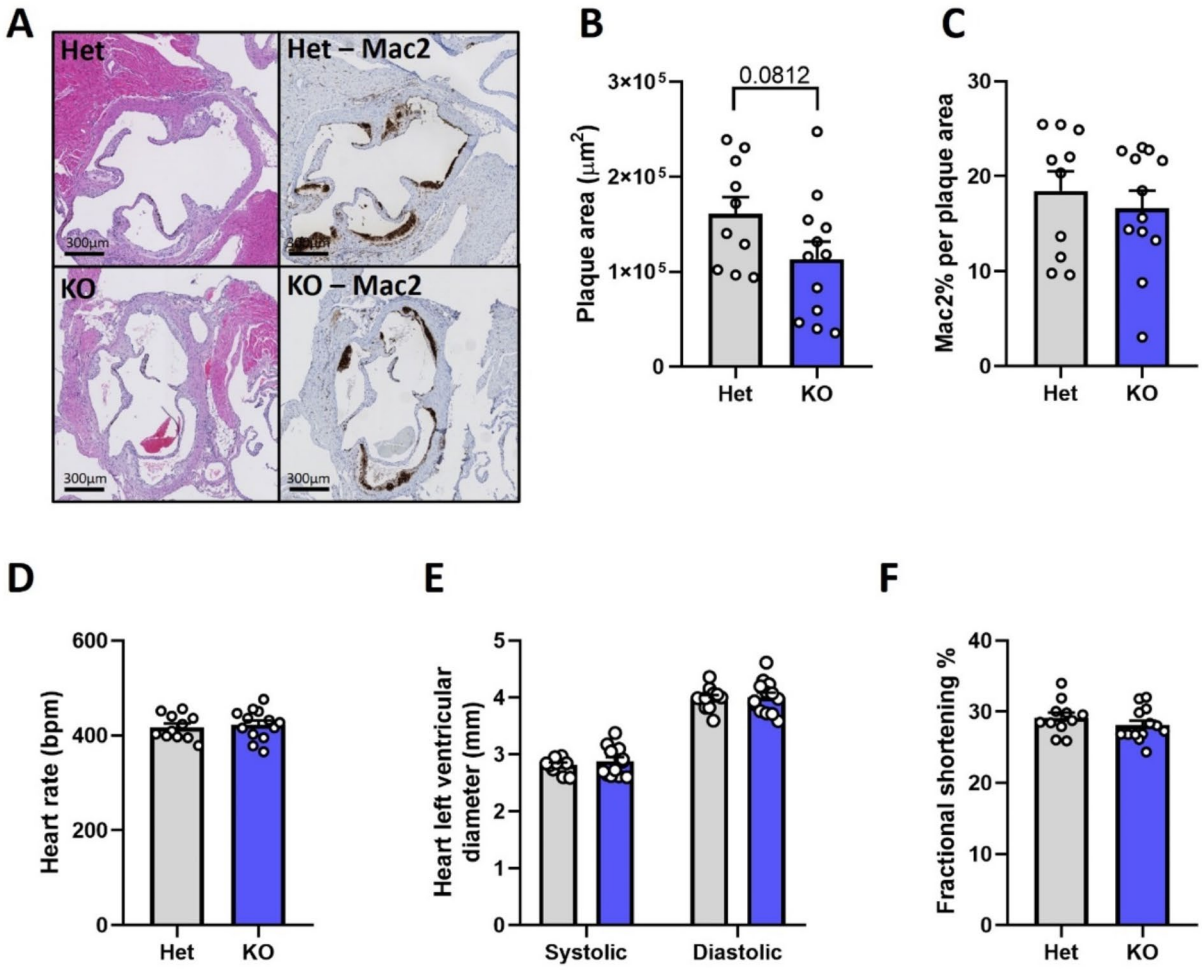


**Fig. 4**. Atherosclerotic plaque size and heart function were not affected in *Cyp2c70*$^{-/-}$ mice. **(A)** Representative of haematoxylin and eosin-stained sections and MAC2$^{+}$ stained sections of the aortic root of *Cyp2c70*$^{-/-}$ and *Cyp2c70*$^{+/-}$ mice after 12 weeks of WD feeding. **(B)** Quantification of atherosclerotic root lesions area. **(C)** Quantification of MAC2$^{+}$ area in atherosclerotic lesions. Echocardiographic analysis, including heart rate **(D)**, left ventricular end-diastolic and end-systolic internal diameters **(E)** and fractional shortening **(F)** in *Cyp2c70*$^{-/-}$ and *Cyp2c70*$^{+/-}$ mice after 12 weeks of WD feeding. Data represent mean ± SEM ($n$ = 10–13 per group).

of unconjugated CDCA[17]. Indeed, on top of high amounts of hydrophobic BA species, we observed an increase in the concentration of unconjugated CDCA in *Cyp2c70*$^{-/-}$ mice (Fig. 1E). Although hepatic inflammation was not measured in our study, liver damage markers were significantly elevated in plasma of *Cyp2c70*$^{-/-}$ mice compared to controls, indicative of hepatic inflammation. Thus, our data indicates that the BA pool of *Cyp2c70*$^{-/-}$ mice exhibits an increased hepatic cytotoxic potential compared to the BA pool of *Cyp2c70*$^{+/-}$ mice, implying that inflammation may have played a role in downregulating *Cyp7a1* and *Cyp8b1* in *Cyp2c70*$^{-/-}$ mice.

We observed lower plasma cholesterol and a (tendency of) triglycerides as well as reduced VLDL-cholesterol levels in *Cyp2c70*$^{-/-}$ mice. Studies have shown that VLDL levels are strong predictors of aortic root atherosclerosis in *Ldlr*$^{-/-}$mice[18,19]. In addition, elevated triglyceride-rich lipoproteins compromise the major pattern of lipid abnormality in patients with atherosclerosis[20], suggesting that the risk factor profile should focus on VLDL- in addition to LDL-cholesterol as causal in atherosclerosis[21]. Unexpectedly, studies have shown elevated plasma LDL cholesterol levels in chow-fed *Cyp2c70*$^{-/-}$mice of both sexes, conceivably due to decreased LDLR protein[9,22]. Since de Boer et al. also observed increased fibrosis and endoplasmic reticulum (ER) stress in the liver, they hypothesized that the elevated ER stress could have caused decreased LDLR protein levels in the liver, thereby increasing plasma LDL cholesterol in *Cyp2c70*$^{-/-}$ mice[9]. In line with our data, Li et al. found a tendency towards lower plasma total cholesterol levels in male *Cyp2c70*$^{-/-}$mice fed 12 weeks of WD[15]. They also observed a reduction in 12α- hydroxylated BAs in *Cyp2c70*$^{-/-}$mice. The ratio of 12α/non-12α-hydroxylated BAs in bile positively correlated with intestinal fat absorption and hepatic lipid concentrations[15]. Since hepatic lipid levels were significantly reduced in our study, the reduced ratio of 12α/non-12α-hydroxylated BAs in bile

of *Cyp2c70*$^{-/-}$ mice may thus be indicative of impaired fat absorption, thereby reducing plasma cholesterol levels in this current study.

Analysing circulating immune cells revealed no significant effects on WBCs counts in male PCSK9-GOF and WD-fed *Cyp2c70*$^{-/-}$ mice. Nevertheless, we observed a reduced percentage of circulating monocytes in *Cyp2c70*$^{-/-}$ mice compared to controls. De Boer et al. reported increased WBCs in chow-fed female *Cyp2c70*$^{-/-}$ mice[9]. They observed a stronger liver phenotype with bridging fibrosis in female *Cyp2c70*$^{-/-}$mice compared to male mice, potentially caused by a decreased ratio of 12α/non-12α-hydroxylated BAs[9]. The exacerbated liver damage could have caused the elevation of circulating WBCs in female mice. As the mice used in this current study were all male, with only minimal fibrosis, WBC counts remained unaffected in *Cyp2c70*$^{-/-}$ mice. With opposing effects of *Cyp2c70*-deletion on risk factors of CVD (increased liver damage versus lower hepatic and plasma lipid levels and circulating monocytes percentages), we investigated the effect of a human-like BA pool on atherosclerosis development and heart function. Analysis of atherosclerotic plaques in the aortic root demonstrated a trend towards smaller plaques in *Cyp2c70*$^{-/-}$ mice compared to controls ($p = 0.08$). Interestingly, previous studies have shown beneficial effects of BA receptor agonists on atherosclerosis development in *Ldlr*$^{-/-}$ mice[7,8]. For example, semisynthetic BA-induced TGR5 activation in macrophages appeared to inhibit atherosclerosis by reducing macrophage inflammation and lipid loading[8]. Miyazaki-Anzai et al. also showed that semisynthetic BA-induced FXR activation leads to anti-inflammatory effects, resulting in reduced atherosclerosis in *Ldlr*$^{-/-}$ mice[7]. Hydrophobic BAs are, in general, stronger activators of FXR and TGR5 than hydrophilic BAs[16], suggesting more BA receptor activation in *Cyp2c70*$^{-/-}$ mice. In this study, the number of pro-inflammatory macrophages in the atherosclerotic plaques remained unaffected upon *Cyp2c70* depletion. Nevertheless, increased BA receptor signaling could have resulted in the lipid-lowering effects (i.e., reduced plasma total cholesterol, triglycerides- and VLDL levels), thereby explaining why we observed a tendency towards smaller plaque lesions in *Cyp2c70*$^{-/-}$ mice. Of note, we cannot exclude a role for the gut microbiota as contributors to the lipid-lowering effects seen in *Cyp2c70*$^{-/-}$ mice. Indeed, we have recently shown that loss of CYP2C70 is associated with a reduced abundance in the genera of *Akkermansia*, *Rikinella* and *Cristensenellaceae*, while *Prevotella* and *Veillonella* are more abundant compared to background-matched WT littermates[9]. We did not analyse the composition of the gut microbiota in PCSK9-GOF *Cyp2c70*$^{-/-}$ and *Cyp2c70*$^{+/-}$ mice after 12 weeks of WD feeding, and in dept mechanistic studies involving fecal microbiota transplantations are needed to understand the impact of these gut microbial alterations in *Cyp2c70*$^{-/-}$mice as well as investigate the role of other microbiota-mediated metabolites implicated in atherogenesis (i.e. short-chain fatty acids)[4].

In humans with obesity there is a large inter-individual variability in plasma BA profiles, with some subjects having mainly CDCA-derived BAs, while others showed a preponderance of CA-derived BAs in plasma[23]. Unexpectedly, secondary BAs deoxycholic acid (DCA) and lithocholic acid (LCA), which are strong BA receptor activators, positively correlated with diabetes and liver fat content[23]. Thus, in contrast to preclinical studies, strong BA receptor activators in the plasma BA pool are associated with risk factors of CVD in humans.

As previously reviewed, studies have shown modulating roles of BAs in cardiovascular function[4]. Activation of FXR, TGR5 and/or muscarinic receptors in cardiomyocytes and/or endothelial cells mostly leads to vasodilatory effects[4]. The hydrophobicity of BAs plays an important role in the magnitude of receptor activation, with hydrophobic BAs being stronger activators. Despite the increased hydrophobicity of the BA pool of *Cyp2c70*$^{-/-}$mice, heart parameters were unaffected in this model. Human studies have shown inconsistencies regarding the association between BAs and CAD[24–27]. The effect of BAs on heart function and its physiological relevance remains therefore unclear.

Although the hydrophobicity of the BA pool in *Cyp2c70*$^{-/-}$ mice resembles that of humans much closer than that of WT mice, substantial differences in BA composition between *Cyp2c70*$^{-/-}$mice and humans still exist. The gut microbiota converts CA and CDCA into DCA and LCA, respectively[5]. In contrast to humans, mice express the CYP2A12 enzyme that re-hydroxylates DCA and LCA into CA and CDCA upon their return in the liver, making the BA pool slightly more hydrophilic[17]. Re-hydroxylating secondary BAs back to primary BAs strongly affects the composition of the BA pool, which also changes the FXR/TGR5 activating potency. Honda et al. simultaneously knocked out both CYP2C70 and CYP2A12 in mice, leading to an even more humanized BA composition compared to CYP2C70 knockout mouse models[17]. Hence, it would be worthwhile to investigate the effect of CYP2C70- and CYP2A12 double knockout on atherogenesis in *Ldlr*$^{-/-}$ or apolipoprotein E knockout (*ApoE*$^{-/-}$)mice. In addition, while humans have both taurine- and glycine-conjugated BAs, mice exclusively have taurine-conjugated BAs. The difference in hydrophobicity between glycine- and taurine-conjugated BAs is, however, minimal, and FXR activation appears to be similar[28]. Whether atherogenesis could be impacted in *Cyp2c70*$^{-/-}$mice expressing human BA conjugating enzymes remains to be investigated. Species differences in BA metabolism between mice and humans may also be related to small differences in FXR structure[29]. Cui et al. have shown that CDCA activates human FXR with a 10-fold higher affinity and 3-fold higher maximal response compared to murine FXR[29]. Different amino acids in the ligand-binding domain of FXR cause this masked species difference. Replacements of Lysine 366 and Valine 384 in murine FXR with Asparagine and Isoleucine, respectively, increased both potency and maximal response to CDCA[29]. Future studies should investigate the effect of human FXR on atherosclerosis development and heart function in *Ldlr*$^{-/-}$ or *ApoE*$^{-/-}$ mice.

Here we used the PCSK9-AAV model to downregulate the LDLR and induce atherosclerosis to investigate the impact of a humanized BA profile on early plaque development in *Cyp2c70*$^{-/-}$ mice fed a WD for 12 weeks. We observed a marginal trend towards decreased atherosclerosis which may be explained by the small lesion sizes in our mice. To overcome this limitation, future studies should include a longer WD intervention when applying the PCSK9-GOF-AAV model to study atherosclerosis. Studying the impact of CYP2C70 knockdown or overexpression in *Ldlr*$^{-/-}$ or *ApoE*$^{-/-}$ mice would be an alternative approach to provide more definitive data to clarify the role of hydrophobic BAs on atherosclerosis disease risk.

In conclusion, male WD-fed *Cyp2c70*$^{-/-}$ mice with a PCSK9-GOF showed a tendency towards smaller atherosclerotic lesions in the initiation phase of the disease, with no overt effects on heart function. Reduced total hepatic and plasma cholesterol, (a tendency of) triglycerides and VLDL-cholesterol levels in *Cyp2c70*$^{-/-}$ mice could potentially explain these results.

## Methods and materials

All methods were performed in accordance with the relevant guidelines and regulations.

### Animals

*Cyp2c70*$^{-/-}$ (KO) and *Cyp2c70*$^{+/-}$ (Het) mice (C57BL/6J-Cyp2c70$^{+/-}$)[9]were generated as previously described[9] and bred in the animal facility of the University Medical Center Groningen. All animal experiments were approved by the Dutch Central Committee for Animal Experiments and the Animal Welfare Body of the University of Groningen. Male KO and Het mice were injected via the orbital vein with $1.0 \times 10^{11}$vector genomes of PCSK9-GOF-AAV[30]at 17–22 weeks at age. Retro-orbital injections are suitable for all murine ages, including older mice[31], and the same *PCSK9-GOF-AAV* model has recently been applied to 7- and 19-month-old C57BL6 mice[32]. Mice were individually housed in a temperature-controlled room (21 °C) with a 12-hourslight/12-hours dark cycle and ad libitum access to food and water. Directly after virus injection mice were fed a Western diet (D11111701-1.5; 45% kcal% Fat and 0.21% Cholesterol; Research Diets Inc, NJ, US) for 12 weeks. At the end of the experiment, body composition was measured in conscious mice, using a Minispec Body Composition Analyzer (LF90; Bruker Bio-Spin GmbH, Germany). Prior to sacrifice by cardiac puncture, four hours fasted mice were anesthetized with Hypnorm (fentanyl/fluanisone; 1 ml/kg) and diazepam (10 mg/kg), after which the bile duct was ligated and the gallbladder cannulated. Mice were then placed into a humidified incubator to maintain body temperature, and bile was collected continuously for 30 min. Bile production was determined gravimetrically. Blood was collected and centrifuged in EDTA-containing tubes, and plasma was stored at −80 C for further analysis. Livers and hearts were dissected, weighted, and fixed in formalin or snap-frozen in liquid nitrogen and stored at −80 °C. The study is reported in accordance with the ARRIVE guidelines and conforms to its principles.

### Western blot

For Western blot, total cell lysates and liver homogenates were obtained using NP40 buffer (0.1% Nonidet P-40 (NP-40), 0.4 M NaCl, 10 mM Tris-HCl (pH 8.0), 1 mM EDTA), freshly supplemented with protease and phosphatase inhibitors (Roche, Switzerland). Protein concentration was determined using the Bradford assay (Bio-Rad, CA, US). 25 mg of protein was separated using sodium dodecyl sulfate polyacrylamide gel electrophoresis (SDS-PAGE) and transferred to Amersham™ Hybond™-P PVDF Transfer Membrane (GE Healthcare, IL, US). Membranes were blocked in 5% milk in tris-buffered saline with 0.01% Tween20 and incubated with rabbit anti-LDLR (1:1000, PAB8804, Abnova GmbH, Germany) and mouse anti-beta-actin (1:5000 A5441, Sigma-Aldrich, MO, US). Proteins were visualized using a ChemiDoc™ XRS + System (Bio-Rad) using Image Lab software version 5.2.1 (Bio-Rad).

### Measurement of bile acids

BAs in plasma and bile were measured by ultra high-performance liquid chromatography-tandem mass spectrometry (UHPLC-MS/MS) on a Nexera X2 UHPLC system (Shimadzu, Kyoto, Japan), coupled to a SCIEX QTRAP 4500 MD triple quadrupole mass spectrometer (SCIEX, MA, US) and quantified using D4-labeled BAs as internal standards[33].

### Plasma parameters

Plasma triglycerides (Roche Diagnostics, Switzerland) and total cholesterol (DiaSys Diagnostic Systems, Germany) were determined by commercially available kits. Plasma lipoproteins were separated by fast protein liquid chromatography (FPLC) using a system containing a PU-4180 pump with linear degasser and UV-4075 UV/VIS detectors (Jasco, Tokyo, Japan), as described[34]. Plasma transaminases were analysed using a Cobas 6000 analyser with standard reagents (Roche Diagnostics, Switzerland).

### Liver lipids

Lipids were extracted from liver homogenates (15% w/w in PBS) according to Bligh and Dyer[35] and subsequently dissolved in 2% TX100 to determine triglycerides, and cholesterol concentrations. Total and free cholesterol was determined using a colorimetric assay, and cholesterol standard FS was used as a reference (DiaSys Diagnostic Systems, Germany). Cholesteryl ester was determined by subtracting the value of free cholesterol from the total cholesterol. Triglyceride levels were measured using a Trig/GB kit, and Precimat Glycerol standard was used as a reference (Roche, Switzerland).

### Real-time quantitative polymerase chain reaction

Real-time quantitative polymerase chain reaction (qPCR) was performed on reverse transcribed RNA using SYBR green mastermix (Roche Diagnostics, Switzerland). Data were normalized to cyclophilin A as a housekeeping gene. Primer sequences were either obtained from previous studies or generated in-house with Primer 3 (https://primer3.ut.ee/) and listed in Supplemental Table S1.

### Histology

Livers and hearts were formalin-fixed in 4% phosphate buffered paraformaldehyde and paraffin-embedded. Liver sections were stained with hematoxylin and eosin (H&E) and Sirius Red/Fast green. Images were obtained

using a Hamamatsu NanoZoomer (Hamamatsu Photonics, Japan). Hearts were cross-sectioned throughout the aortic root area (4 µm sections) and stained with H&E or MAC2 (Galectin-3). Lesion size was quantified blindly in H&E-stained sections by morphometric analysis using Image Scope (Leica Biosystems Aperio, CA, US). Lesion size was presented as the average taken from 4 sections per heart as previously described[36]. For MAC2 staining paraffin sections were incubated in a preheated citric acid-based buffer (H-3300, Vector Laboratories, CA, US) for 15 min and cooled down for 30 min. Sections were then blocked in 10% goat serum for 30 min at RT and incubated overnight at 4 °C with rat anti-mouse/human MAC2 primary antibody (1/5000 dilution, Cedarlane, Canada). Sections were subsequently stained with biotinylated goat anti-rat secondary antibody for 30 min at RT (1:125 dilution) and Vectastain ABC-peroxidase kit according to the manufacturer's instructions, followed by staining with diaminobenzidene (DAB) for 10 min at RT and counterstaining with haematoxylin.

### Echocardiography

Echocardiographic measurements were performed using a Vevo 3100 preclinical imaging system, equipped with a 40-MHz MX550D linear array transducer (FUJIFILM VisualSonics, Canada). Left-ventricular (LV) short axis M-mode recordings were obtained at the mid-papillary level. Vevo LAB software (version 5.7.1; FUJIFILM VisualSonics) was used to determine heart rate, LV end-diastolic internal diameter (LVIDd), LV end-systolic internal diameter (LVIDs) and fractional shortening (FS) by outlining the epicardial and endocardial borders using the LV Trace tool. For all measurements, three subsequent cardiac cycles, unaffected by respiration, were analysed.

### Flow cytometry

At ten weeks of WD feeding, blood samples were collected by tail bleeding into heparin capillaries and WBC count was determined by CBC (Medonic CA 620, Bimedis, Ukraine). For analysis of blood leukocytes, red blood cells were lysed (BD pharm Lyse, BD Biosciences) and WBCs were stained with a cocktail of antibodies against CD45-APC-Cy7 (557659, BD Biosciences), CD115-APC (17–1152-80, eBioscience) and Ly6C/G-PerCP-Cy5.5 (561103, BD Biosciences) as described in Westerterp et al.[36]. Neutrophils were identified as $CD45^{+}CD115^{-}Ly6G^{+}$ and monocytes as $CD45^{+}CD115^{+}$. Monocytes were further identified as $Ly6C^{low}$ and $Ly6C^{high}$ subsets. Flow cytometry measurements were performed on NovoCyte Quanteon (Agilent, CA, US) and analysed using NovoExpress (version 1.6.2) software.

### Statistics

All data are presented as mean ± standard errors of the mean (SEM). Statistical analysis was performed using GraphPad Prism 9 Software (Graphpad Software, CA, US). All data were tested for normality by d'Agastino and Pearson normality test. For normally distributed data, Student's T-test was used. For non-normally distributed data, non-parametric Mann-Whitney U test was used. Data was considered significant if $p < 0.05$.

## Data availability

The dataset that support the findings of this study have been deposited in Harvard Dataverse: https://doi.org/10.7910/DVN/TAEUOA.

Received: 9 April 2024; Accepted: 8 January 2025
Published online: 15 January 2025

## References

1. *Cardiovascular Diseases (CVDs)*. (2021). https://www.who.int/news-room/fact-sheets/detail/cardiovascular-diseases-(cvds)
2. Libby, P. et al. Atherosclerosis. *Nat. Rev. Dis. Primers.* **5**, 56 (2019).
3. Soehnlein, O. & Libby, P. Targeting inflammation in atherosclerosis — from experimental insights to the clinic. *Nat. Rev. Drug Discov.* **20**, 589–610 (2021).
4. Yntema, T., Koonen, D. P. Y. & Kuipers, F. Emerging roles of gut microbial modulation of bile acid composition in the etiology of Cardiovascular diseases. *Nutrients* **15**, 1850 (2023).
5. Wahlström, A., Sayin, S. I., Marschall, H. U. & Bäckhed, F. Intestinal crosstalk between bile acids and microbiota and its impact on host metabolism. *Cell. Metab.* **24**, 41–50 (2016).
6. Charach, G. et al. Diminished bile acids excretion is a risk factor for coronary artery disease: 20-year follow up and long-term outcome. *Th. Adv. Gastroenterol.* **11**, 1756283X17743420 (2018).
7. Miyazaki-Anzai, S. et al. Simultaneous inhibition of FXR and TGR5 exacerbates atherosclerotic formation. *J. Lipid Res.* **59**, 1709–1713 (2018).
8. Pols, T. W. H. et al. TGR5 activation inhibits atherosclerosis by reducing macrophage inflammation and lipid loading. *Cell. Metab.* **14**, 747–757 (2011).
9. de Boer, J. F. et al. Cholangiopathy and biliary fibrosis in Cyp2c70-Deficient mice are fully reversed by Ursodeoxycholic Acid. *CMGH* **11**, 1045–1069 (2021).
10. Yang, J., Palmiotti, A. & Kuipers, F. Emerging roles of bile acids in control of intestinal functions. *Curr. Opin. Clin. Nutr. Metab. Care.* **24**, 127–133 (2021).
11. Sayin, S. I. et al. Gut microbiota regulates bile acid metabolism by reducing the levels of tauro-beta-muricholic acid, a naturally occurring FXR antagonist. *Cell. Metab.* **17**, 225–235 (2013).
12. Lefebvre, P., Cariou, B., Lien, F., Kuipers, F. & Staels, B. Role of bile acids and bile acid receptors in metabolic regulation. *Physiol. Rev.* **89**, 147–191 (2009).
13. Heuman', D. M. Quantitative estimation of the hydrophilic-hydrophobic balance of mixed bile salt solutions. *J. Lipid Res.* **30**, 719–730 (1989).
14. El Hadi, H., Di Vincenzo, A., Vettor, R. & Rossato, M. Relationship between Heart Disease and Liver Disease: a two-Way Street. *Cells* **9**, 567 (2020).
15. Li, R. et al. Low production of 12α-hydroxylated bile acids prevents hepatic steatosis in Cyp2c70-/- mice by reducing fat absorption. *J. Lipid Res.* **62**, (2021).

16. Li, R., Andreu-Sánchez, S., Kuipers, F. & Fu, J. Gut microbiome and bile acids in obesity-related diseases. *Best Pract. Res. Clin. Endocrinol. Metab.* **35**, 101493 (2021).
17. Honda, A. et al. Regulation of bile acid metabolism in mouse models with hydrophobic bile acid composition. *J. Lipid Res.* **61**, 54–69 (2020).
18. Nakajima, K. & Tanaka, A. Atherogenic postprandial remnant lipoproteins; VLDL remnants as a causal factor in atherosclerosis. *Clin. Chim. Acta*. **478**, 200–215 (2018).
19. VanderLaan, P. A., Reardon, C. A., Thisted, R. A. & Getz, G. S. VLDL best predicts aortic root atherosclerosis in LDL receptor deficient mice. *J. Lipid Res.* **50**, 376–385 (2009).
20. Nordestgaard, B. G. & Varbo, A. Triglycerides and cardiovascular disease. *Lancet* **384**, 626–635 (2014).
21. Libby, P. The changing landscape of atherosclerosis. *Nature* **592**, 524–533 (2021).
22. Straniero, S. et al. Of mice and men: murine bile acids explain species differences in the regulation of bile acid and cholesterol metabolism. *J. Lipid Res.* **61**, 480–491 (2020).
23. Chen, L. et al. Genetic and Microbial associations to plasma and fecal bile acids in obesity relate to plasma lipids and liver Fat Content. *Cell. Rep.* **33**, (2020).
24. Chong Nguyen, C. et al. Circulating bile acids concentration is predictive of coronary artery disease in human. *Sci. Rep.* **11**, 22661 (2021).
25. Li, W. et al. Fasting serum total bile acid level is associated with coronary artery disease, myocardial infarction and severity of coronary lesions. *Atherosclerosis* **292**, 193–200 (2020).
26. Steiner, C. et al. Bile acid metabolites in serum: intraindividual variation and associations with coronary heart disease, metabolic syndrome and diabetes mellitus. *PLoS One*. **6**, e25006 (2011).
27. Neale, G., Lewis, B., Weaver, V. & Panveliwalla, D. Serum bile acids in liver disease. *Gut* **12**, 145–152 (1971).
28. Reschly, E. J. et al. Evolution of the bile salt nuclear receptor FXR in vertebrates. *J. Lipid Res.* **49** (7), 1577–1587 (2008).
29. Cui, J. et al. The amino acid residues asparagine 354 and isoleucine 372 of human farnesoid X receptor confer the receptor with high sensitivity to chenodeoxycholate. *J. Biol. Chem.* **277**, 25963–25969 (2002).
30. Louloudis, G. et al. Adeno-Associated virus-mediated gain-of-function mPCSK9 expression in the mouse induces hypercholesterolemia, Monocytosis, Neutrophilia, and a hypercoagulative state. *Front. Cardiovasc. Med.* **8**, 718741 (2021).
31. Prabhakar, S. et al. AAV9 transduction mediated by systemic delivery of vector via retro-orbital injection in newborn, neonatal and juvenile mice. *Exp. Anim.* **70** (4), 450–458 (2021).
32. Gogulamudi, V. R. et al. Advancing age increases the size and severity of spontaneous atheromas in mouse models of atherosclerosis. *Geroscience* **45** (3), 1913–1193 (2023).
33. Eggink, H. M. et al. Chronic infusion of taurolithocholate into the brain increases fat oxidation in mice. *J. Endocrinol.* **236**, 85–97 (2018).
34. Gerdes, M. L. U., Gerdes, C., Klausen, C. & Faergeman, O. Generation of analytic plasma lipoprotein profiles using two prepacked superose 6B columns. *Clin. Chim. Acta*. **205**, 1–9 (1992).
35. Bligh, E. G. & Dyer, W. J. A rapid method of total lipid extraction and purification. *Can. J. Biochem. Physiol.* **37**, 911–917 (1959).
36. Westerterp, M. et al. Cholesterol Accumulation in dendritic cells links the Inflammasome to Acquired Immunity. *Cell. Metab.* **25**, 1294–1304 (2017).

## Acknowledgements

We thank the personnel from the Central Animal Facility of the University Medical Center Groningen for their support with the animal experiments.

## Author contributions

FK and DK conceived and designed the study. TY, TE, NK, RH, MK, MH, DK carried out the experiments (TY, NK, RH, mouse experiments; TE, TY heart echo's; TY, MK, histology; TY, NK, qPCR; RH, MH, JFB, bile acid measurement; DK, lipid measurement. TY, TE, DK, FK wrote the manuscript. All others critically reviewed the manuscript and approved the final version.

## Funding

This work was funded by the Netherlands Heart Foundation to F. Kuipers and D. Koonen (IN-CONTROL II, CVON grant 2018-27).

## Declarations

## Competing interests

The authors declare no competing interests.

## Additional information

**Supplementary Information** The online version contains supplementary material available at https://doi.org/10.1038/s41598-025-86183-9.

**Correspondence** and requests for materials should be addressed to D.P.Y.K.